Slip flow on Stagnation Point over a Stretching Sheet in a Viscoelastic Nanofluid

M.K.A. Mohamed[1,a)*], N.A.Z. Noar[1,b)], M.Z. Salleh[1,c)] and A. Ishak[2,d)]

[1]*Applied & Industrial Mathematics Research Group,*
Faculty of Industrial Sciences & Technology, Universiti Malaysia Pahang,
26300 UMP Kuantan, Pahang, Malaysia.
[2]*School of Mathematical Sciences, Faculty of Science and Technology,*
Universiti Kebangsaan Malaysia,43600 UKM Bangi, Selangor, Malaysia.

[a)]baa_khy@yahoo.com, [b)]aidaz@ump.edu.my, [c)]zukikuj@yahoo.com, [d)]anuar_mi@ukm.edu.my

Abstract. In this study, the numerical investigation of stagnation point flow past a stretching sheet immersed in a viscoelastic (Walter's liquid-B model) nanofluid with velocity slip condition and constant wall temperature is considered. The governing equations for the model which is non linear partial differential equations are first transformed by using similarity transformation. Then, the Runge-Kutta-Fehlberg method is employed to solve the transformed ordinary differential equations. Numerical solutions are obtained for the reduced Nusselt number, the Sherwood number and the skin friction coefficient. Further, the effects of slip parameter on the Nusselt number and the Sherwood number are analyzed and discussed. It is found that the heat and mass transfer rate is higher for the Walter's fluid compared to the classical viscous fluid and the presence of the velocity slip reduces the effects of the stretching parameter on the skin friction coefficient.

Keywords: Nanofluid, Slip conditions, Stagnation point flow, Stretching sheet, Viscoelastic Walter's liquid-B model.
PACS: 44.20.+b, 44.25.+f, 44.27.+g

INTRODUCTION

The study on convection boundary layer flow over a stretching sheet started since early of 70's. It is due to a numerous and important applications in polymer processing industry which later corroborated with non-Newtonian fluid like the viscoelastic fluid and also the nanofluid. For instant, it is used in the manufacturing process of artificial film, artificial fibers, polymer extrusion, drawing of plastic films and wire, glass fiber and paper production, manufacture of foods, crystal growing and liquid films in condensation process [1]. The quality of the final product depends to a large extent on the stretching rate and the rate of heat transfer on the stretching sheet.

Crane [2] was the first to study the forced convection boundary layer flow over a stretching sheet. Then Gupta and Gupta [3] updated this topic with the suction and blowing effects. The temperature and concentration distributions are obtained regarding the flow on isothermal moving plate. Chiam [4] considered the study on stagnation point flow over a stretching sheet. This configuration then have been extended to other type of fluids like viscoelastic fluid, micropolar fluid, Casson fluid, Maxwell fluid as well as the nanofluid. Nazar et al. [5] and Ishak et al. [6, 7] considered micropolar fluid in their study while Abbas et al. [8] and Motsa et al. [9] focused on stagnation flow in Maxwell fluid. The study on Casson fluid, second grade fluid and Walter's fluid have been done by Ariel et al. [10], Hayat et al. [11, 12] and Mohamed et al. [13], respectively while the nanofluid stagnation point flow past a stretching sheet have been discussed by Nazar et al. [14], Bachok et al. [15], Kameswaran et al. [16] and recently by Mohamed et al. [17] and Sulochana and Sandeep [18].

In considering the slip effects, researchers have classified the slip flow into a several type for example the partial slip, temperature slip flow, the first order and second order slip flow. These configurations disobey the no slip conditions. Noticed that in no slip conditions, the fluid come in contact with surface body did not have any relative velocity (Prabhakara and Deshpande [19]). According to Bhattacharyya et al. [20], the no slip assumptions is not applicable for all cases of fluid flow. It is due to some situations where the no slip conditions may be replaced with partial or slip condition. Recent studies consider the slip effects onto study on stretching flow includes Nandy and Mahapatra [21], Das [22], Malvandi et al. [23] and Hashim et al. [24].

Motivated from the above literature, present study consider the slip flow on stagnation point past a stretching sheet immersed in viscoelastic nanofluid. Such study is never been considered before, hence the results discussed are new.

MATHEMATICAL FORMULATION

Consider a steady laminar boundary layer stagnation-point flow over a stretching surface immersed in a viscoelastic nanofluid of ambient temperature, T_∞. Two-dimensional rectangular Cartesian coordinates (x, y) are applied, in which the x-axis taken as the coordinate parallel to the plate while y-axis measure from the plate surface normal to it. The physical model and the coordinate system are shown in Fig. 1. It is assumed that T is the temperature, T_w is the wall temperature, $u_e(x)$ is the external velocity and $\varepsilon u_w(x)$ is the stretching velocity where ε is constant stretching $(\varepsilon > 0)$ or shrinking $(\varepsilon < 0)$ parameter. Also, C, C_w and C_∞ are taken as nanoparticle volume fraction, ambient and wall nanoparticle volume fraction, respectively. Following Buongiorno [25], the basic steady continuity, momentum, energy and concentration equations for nanofluid are given as follows [10, 16, 17, 13]:

$$\frac{\partial u}{\partial x} + \frac{\partial v}{\partial y} = 0, \tag{1}$$

$$u\frac{\partial u}{\partial x} + v\frac{\partial u}{\partial y} = u_e\frac{d u_e}{d x} + \nu\frac{\partial^2 u}{\partial y^2} - \frac{k_0}{\rho}\left(u\frac{\partial^3 u}{\partial x \partial y^2} + \frac{\partial u}{\partial x}\frac{\partial^2 u}{\partial y^2} + \frac{\partial u}{\partial y}\frac{\partial^2 v}{\partial y^2} + v\frac{\partial^3 u}{\partial y^3}\right) \tag{2}$$

$$u\frac{\partial T}{\partial x} + v\frac{\partial T}{\partial y} = \frac{k}{\rho C_p}\frac{\partial^2 T}{\partial y^2} + \tau\left[D_B\frac{\partial C}{\partial y}\frac{\partial T}{\partial y} + \frac{D_T}{T_\infty}\left(\frac{\partial T}{\partial y}\right)^2\right], \tag{3}$$

$$u\frac{\partial C}{\partial x} + v\frac{\partial C}{\partial y} = D_B\frac{\partial^2 C}{\partial y^2} + \frac{D_T}{T_\infty}\frac{\partial^2 T}{\partial y^2}, \tag{4}$$

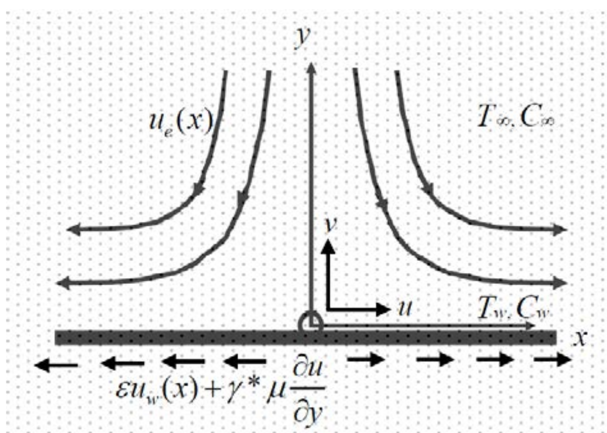

FIGURE 1. Physical model and the coordinate system

subject to the boundary conditions

$$u=\varepsilon u_w(x)+\gamma^*\mu\frac{\partial u}{\partial y},\ v=0,\ T=T_w,\ C=C_w \text{ at } y=0,$$
$$u=u_e(x),\qquad T\to T_\infty,\qquad C\to C_\infty \text{ as }\qquad y\to\infty, \tag{5}$$

where *u* and *v* are the velocity components along the x and y directions, respectively. ν is the kinematic viscosity, μ is the dynamic viscosity, ρ is the fluid density, k is the thermal conductivity, k_0 is the viscoelastic parameter and C_p is the specific heat capacity at a constant pressure. Furthermore, γ^* is the velocity slip factor, D_B is the Brownian diffusion coefficient, D_T is the thermophoresis diffusion coefficient and τ is the ratio of the effective heat capacity of the nanoparticle material and the heat capacity of the fluid. It is also assume that $u_e(x)=u_w(x)=ax,$ where a is a positive constant.

Next, it is consider the similarity variables:

$$\eta=\left(\frac{a}{\nu}\right)^{1/2}y\,,\ \ \psi=\left(a\nu\right)^{1/2}xf(\eta)\,,\quad \theta(\eta)=\frac{T-T_\infty}{T_w-T_\infty},\ \phi(\eta)=\frac{C-C_\infty}{C_w-C_\infty}, \tag{6}$$

where η and ψ are dimensionless variable and stream function for the transform ordinary differential equation which is defined as $u=\frac{\partial\psi}{\partial y}$ and $v=-\frac{\partial\psi}{\partial x}$ and identically satisfy Eq. (1). Furthermore, ϕ and θ are the rescaled dimensionless nanoparticle volume fraction and temperature of the fluid, respectively. From the definition of *u* and *v* above, it is obtained

$$u=axf'(\eta),\ v=-(a\nu)^{1/2}f(\eta). \tag{7}$$

By substituting Eqs. (6) and (7) into Eqs. (2)-(4) give

$$f'''+ff''+1-f'^2+K(ff^{iv}-2ff'''+f''^2)=0 \tag{8}$$

$$\frac{1}{\Pr}\theta''+f\theta'+N_b\theta'\phi'+N_t\theta'^2=0, \tag{9}$$

$$\phi''+\frac{N_t}{N_b}\theta''+Lef\phi'=0 \tag{10}$$

The boundary conditions (5) are transformed to

$$f(0)=0,\ \ f'(0)=\varepsilon+\gamma f''(0),\ \ \theta(0)=1,\ \ \phi(0)=1,$$
$$f'(\eta)\to 1,\ \ \theta(\eta)\to 0,\ \ \phi(\eta)\to 0, \text{ as } y\to\infty \tag{11}$$

where $\Pr=\frac{\nu\rho C_p}{k}$ is the Prandtl number, $N_b=\frac{\tau D_B(C_w-C_\infty)}{\nu}$ and $N_t=\frac{\tau D_T(T_w-T_\infty)}{T_\infty\nu}$ are the Brownian and thermophoresis parameters, $Le=\frac{\nu}{D_B}$ is Lewis number, $K=\frac{a\,k_0}{\rho\nu}$, is a dimensionless viscoelastic parameter and $\gamma=\gamma^*\rho\left(a\nu\right)^{1/2}$ is the velocity slip parameters.

It is worth mentioning that $K>0$ and $K<0$ refer to Walter's and second grade nanofluid, respectively, while $K=0$ is valid for an ordinary incompressible nanofluid. In this study, only the case $K\ge 0$ will be considered. The physical quantities of interest are the skin friction coefficient C_f, the local Nusselt number Nu_x and the local Sherwood number Sh_x which are given by

$$C_f = \frac{\tau_w}{\rho u_w^2}, \qquad Nu_x = \frac{x q_w}{k(T_w - T_\infty)}, \qquad Sh_x = \frac{x j_w}{D_B (C_w - C_\infty)}. \tag{12}$$

The surface shear stress τ_w, the surface heat flux q_w and the surface mass flux j_w are given by

$$\tau_w = \mu\left(\frac{\partial u}{\partial y}\right)_{y=0} - k_0\left(u\frac{\partial^2 u}{\partial x \partial y} - 2\frac{\partial u}{\partial y}\frac{\partial v}{\partial y}\right)_{y=0}, \qquad q_w = -k\left(\frac{\partial T}{\partial y}\right)_{y=0}, \qquad j_w = -D_B\left(\frac{\partial C}{\partial y}\right)_{y=0}, \tag{13}$$

with $\mu = \rho \nu$ and k being the dynamic viscosity and the thermal conductivity, respectively. Using the variables in (6) gives

$$C_f \operatorname{Re}_x^{1/2} = \left[1 - 3Kf'(0)\right] f''(0), \;\; Nu_x \operatorname{Re}_x^{-1/2} = -\theta'(0), \;\; Sh_x \operatorname{Re}_x^{-1/2} = -\phi'(0) \tag{14}$$

where $\operatorname{Re}_x = \frac{u_w x}{\nu}$ is the local Reynolds number.

RESULTS AND DISCUSSION

Equations (8) - (10) with boundary conditions (11) were solved numerically using the Runge-Kutta-Fehlberg method which encoded in MAPLE software for computation. The boundary layer thicknesses in the range of 2 until 7 were adequate for the velocity and the temperature profiles to reach the far field boundary conditions asymptotically. Seven parameters were considered in this study, namely Prandtl number Pr, the dimensionless viscoelastic parameter K, the stretching parameter ε, the Lewis number Le, the velocity slip parameter γ, and the Brownian N_b and thermophoresis motion parameter N_t. The solution was obtained for the reduce Nusselt number $Nu_x \operatorname{Re}_x^{-1/2}$, reduced Sherwood number $Sh_x \operatorname{Re}_x^{-1/2}$ and the reduced skin friction coefficient $C_f \operatorname{Re}_x^{1/2}$.

In order to validate the efficiency of the numerical method used, the comparison with those reported previously has been made. Tables 1 and 2 show the comparison values of $f''(0)$ and $-\theta'(0)$ with previously published results for viscous fluid $(K = 0)$, respectively. The good agreement is seen from both tables which gives a confidence in terms of accuracy of results presented in this study.

TABLE 1. Comparison values of $f''(0)$ with previous results for various values of ε when $\Pr = 1$ and $N_b = N_t = Le = \gamma = K = 0.$

ε	$f''(0)$			
	Wang [26]	Lok et al. [27]	Kameswaran et al. [16]	Present
0	1.232588	1.232588	1.232588	1.2325876
0.1	1.14656	1.146561	1.146561	1.1465610
0.2	1.05113	1.051130	1.051130	1.0511300
1	0.00000	0.000000	0.00000	0.0000000
2	-1.88731	-1.887307	-1.887307	-1.8873068
5	-10.26475	-10.264749	-10.264749	-10.2647493

TABLE 2. Comparison values of $-\theta'(0)$ with previous results for various values of Pr when $K = \varepsilon = N_b = N_t = Le = \gamma = 0$

Pr	Eckert [28]	Salleh et al. [29]	Present
0.7	0.496	0.4959	0.4959
0.8	0.523	0.5228	0.5227
1	0.570	0.5705	0.5705
5	1.043	1.0436	1.0434
7	-	1.1786	1.1784
10	1.344	1.3391	1.3388
100	-	2.9897	2.9863

Table 3 presents the values of $Nu_x \mathrm{Re}_x^{-1/2}$ and $Sh_x \mathrm{Re}_x^{-1/2}$ for various values of ε and K. From table 3, it is found that the presence of stretching effects $(\varepsilon > 0)$ increase the values of $Nu_x \mathrm{Re}_x^{-1/2}$ and $Sh_x \mathrm{Re}_x^{-1/2}$ which physically denoted as the increasing in convective capability in heat and mass transfer, respectively. The trend goes oppositely for the shrinking case $(\varepsilon < 0)$, where ε reduced the values of $Nu_x \mathrm{Re}_x^{-1/2}$ and $Sh_x \mathrm{Re}_x^{-1/2}$. Next, it is concluded that the Walter's fluid $(K > 0)$ provide a better convective heat and mass transfer rate compared to viscous fluid $(K = 0)$. As shown in Table 3, the increase of K enhanced the values of $Nu_x \mathrm{Re}_x^{-1/2}$ and $Sh_x \mathrm{Re}_x^{-1/2}$.

The values of $Nu_x \mathrm{Re}_x^{-1/2}$ and $Sh_x \mathrm{Re}_x^{-1/2}$ for various values of N_b and N_t are tabulated in Table 4. From this table, it can be concluded that the increase of both parameters N_b and N_t results in a decreasing manner of the $Nu_x \mathrm{Re}_x^{-1/2}$. This is due to the higher values of N_b and N_t subsequently results to higher volume of nanoparticles migrating away from the vicinity of the wall, and thus reduces the value of $Nu_x \mathrm{Re}_x^{-1/2}$. Large values of N_b and N_t for example $N_b = 2$ is sufficient to terminated the convective heat transfer and promoted to the pure conduction process $Nu_x \mathrm{Re}_x^{-1/2} = 0$. Meanwhile. $Sh_x \mathrm{Re}_x^{-1/2}$ is increases with the increase of N_b but decreases with N_t.

TABLE 3. Values of $Nu_x \mathrm{Re}_x^{-1/2}$ and $Sh_x \mathrm{Re}_x^{-1/2}$ for various values of ε and K when $N_b = N_t = 0.1$, $Le = 15, \gamma = 0.5$ and Pr = 7.

ε	$K = 0.0$		$K = 1.0$	
	$Nu_x \mathrm{Re}_x^{-1/2}$	$Sh_x \mathrm{Re}_x^{-1/2}$	$Nu_x \mathrm{Re}_x^{-1/2}$	$Sh_x \mathrm{Re}_x^{-1/2}$
-0.75	0.5102	1.4999	0.7386	2.2096
-0.5	0.6063	1.8098	0.8113	2.4384
-0.25	0.6909	2.0773	0.8772	2.6441
0	0.7665	2.3132	0.9340	2.8203
0.5	0.8978	2.7181	1.0372	3.1386
1	1.0099	3.0608	1.1294	3.4212
1.5	1.1082	3.3602	1.2130	3.6765
2	1.1961	3.6275	1.2896	3.9101
5	1.5978	4.8454	1.6559	5.0220

TABLE 4. Values of $Nu_x \mathrm{Re}_x^{-1/2}$ and $Sh_x \mathrm{Re}_x^{-1/2}$ for various values of N_b and N_t when $K = 1$, $Le = 15, \varepsilon = \gamma = 0.5$ and Pr = 7.

N_b	N_t	$Nu_x \mathrm{Re}_x^{-1/2}$	$Sh_x \mathrm{Re}_x^{-1/2}$
0.1	0.5	0.4016	4.5929
0.5	0.5	0.0446	3.5616
1.0	0.5	0.0020	3.3131
2.0	0.5	0.0000	3.2001
0.5	0.1	0.1174	3.2335
0.5	0.5	0.0446	3.5612
0.5	1.0	0.0204	3.7634
0.5	2.0	0.0087	3.9389

Figures 2, 3 and 4 illustrate the variation of $Nu_x \mathrm{Re}_x^{-1/2}, Sh_x \mathrm{Re}_x^{-1/2}$ and $C_f \mathrm{Re}_x^{1/2}$ for various values of K and γ. From figures, it is found that the values of $Nu_x \mathrm{Re}_x^{-1/2}$ and $Sh_x \mathrm{Re}_x^{-1/2}$ increases as K increases while $C_f \mathrm{Re}_x^{1/2}$ do oppositely. This made a Walter's nanofluid as a better lubricants compared to ordinary nanofluid due to its high capability on convective heat transfer besides provided a minimum friction between surfaces. Further, the presence of a velocity slip parameter $(\gamma = 0.5)$ also enhanced the values of $Nu_x \mathrm{Re}_x^{-1/2}$ and $Sh_x \mathrm{Re}_x^{-1/2}$ except for $C_f \mathrm{Re}_x^{1/2}$. The presence of slip effect has reduced the $C_f \mathrm{Re}_x^{1/2}$. It is suggested that the presence of γ provided a drastically changes on the physical quantities discussed and γ effects are more significant at large values of K.

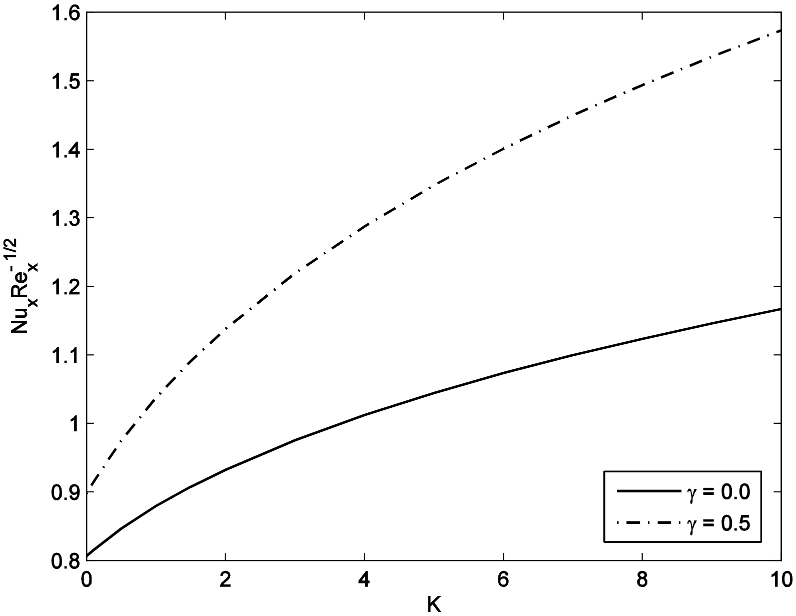

FIGURE 2. Variation of $Nu_x \operatorname{Re}_x^{-1/2}$ for various values of K when $N_b = N_t = 0.1,\ Le = 15, \varepsilon = 0.5$ and $\Pr = 7$.

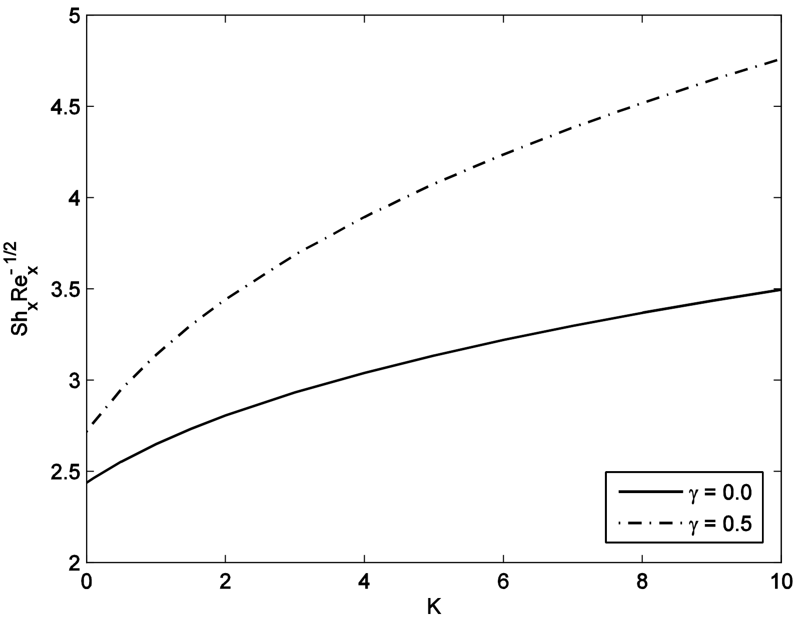

FIGURE 3. Variation of $Sh_x \operatorname{Re}_x^{-1/2}$ for various values of K when $N_b = N_t = 0.1,\ Le = 15, \varepsilon = 0.5$ and $\Pr = 7$.

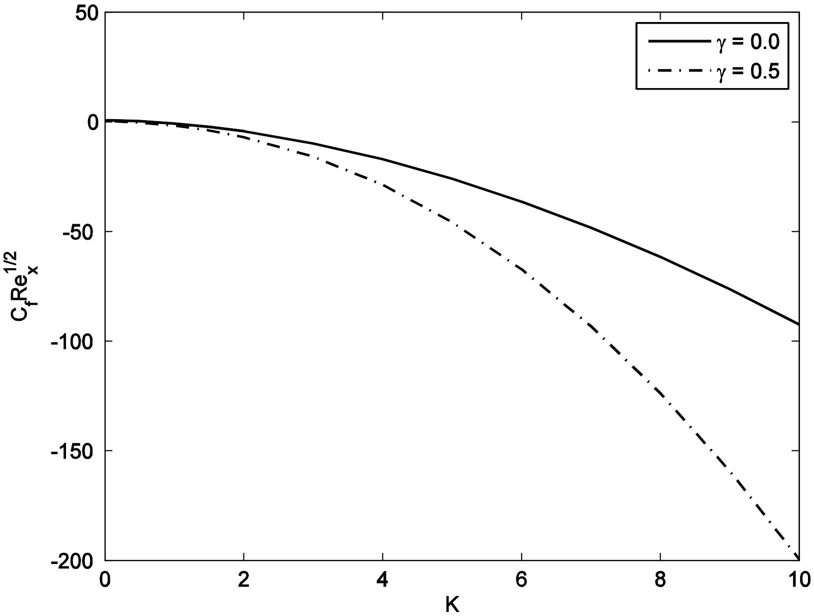

FIGURE 4. Variation of $C_f \mathrm{Re}_x^{1/2}$ for various values of K when $N_b = N_t = 0.1$, $Le = 15, \varepsilon = 0.5$ and $\Pr = 7$.

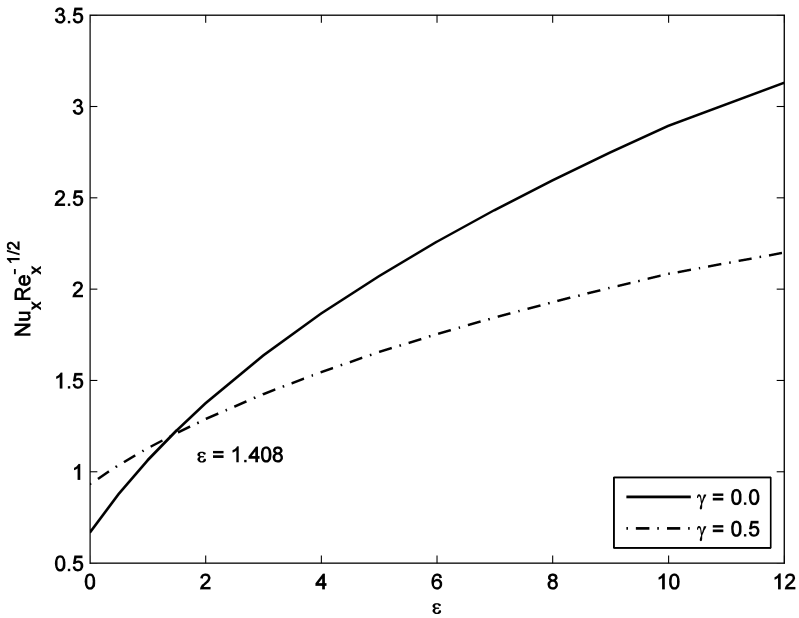

FIGURE 5. Variation of $Nu_x \mathrm{Re}_x^{-1/2}$ for various values of ε when $N_b = N_t = 0.1$, $Le = 15, K = 1$ and $\Pr = 7$.

The variation of $Nu_x \mathrm{Re}_x^{-1/2}, Sh_x \mathrm{Re}_x^{-1/2}$ and $C_f \mathrm{Re}_x^{1/2}$ for various values of ε and γ are shown in Figs. 5, 6 and 7. The effects of ε agreed with K where the values of $Nu_x \mathrm{Re}_x^{-1/2}$ and $Sh_x \mathrm{Re}_x^{-1/2}$ increases as ε increases. Meanwhile, the increase of ε gives the small reduction on $C_f \mathrm{Re}_x^{1/2}$ before increase drastically as ε increases. Next, it is worth mentioning that the changes in variation behavior occur when the velocity slip parameter γ is present. It is noticed that in Figs. 5 and 6, the presence of velocity slip parameter $(\gamma = 0.5)$ enhanced the values of

$Nu_x \mathrm{Re}_x^{-1/2}$ and $Sh_x \mathrm{Re}_x^{-1/2}$ for stretching parameter $\varepsilon \le 1.408$ and $\varepsilon \le 1.414$, respectively. This situation goes oppositely for $\varepsilon \ge 1.408$ and $\varepsilon \ge 1.414$, where the presence of velocity slip $(\gamma = 0.5)$ reduced the values of $Nu_x \mathrm{Re}_x^{-1/2}$ and $Sh_x \mathrm{Re}_x^{-1/2}$, respectively. The presence of γ has accelerated the nanoparticles at the surface from static (no slip) to a certain velocity which results to the reducing in stretching parameter effects, hence reduce the ability in convective heat and mass transfer.

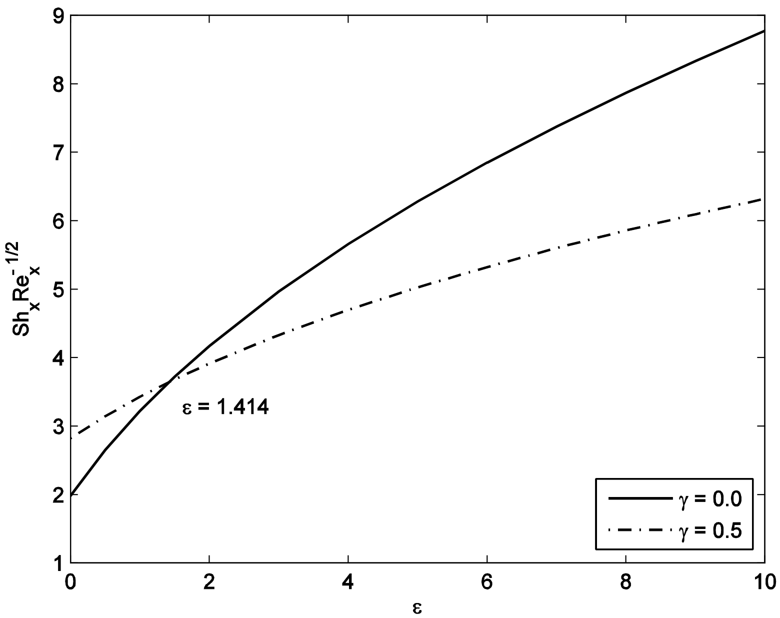

FIGURE 6. Variation of $Sh_x \mathrm{Re}_x^{-1/2}$ for various values of ε when $N_b = N_t = 0.1$, $Le = 15, K = 1$ and $\mathrm{Pr} = 7$.

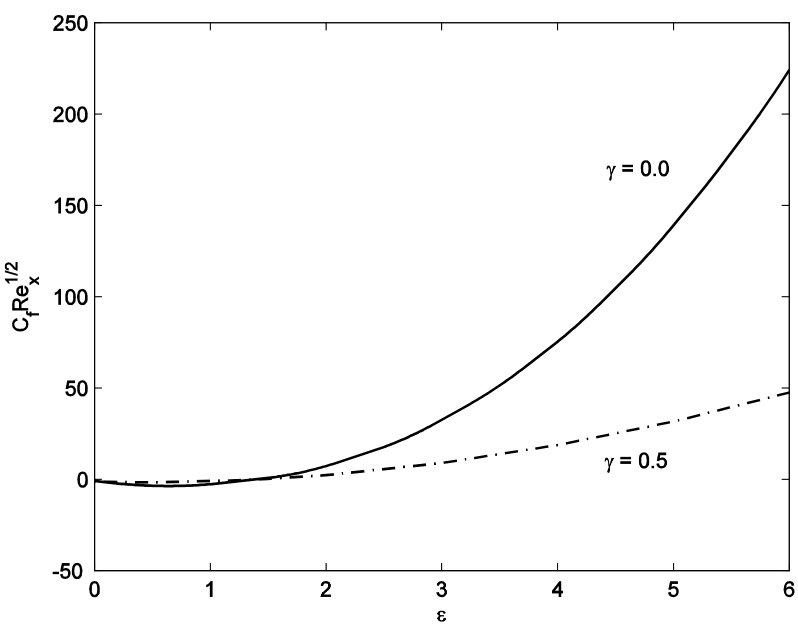

FIGURE 7. Variation of $C_f \mathrm{Re}_x^{1/2}$ for various values of ε when $N_b = N_t = 0.1$, $Le = 15, K = 1$ and $\mathrm{Pr} = 7$.

From Fig. 7, the increase of ε enhanced the velocity gradient from surface to the ambient flow. This situation increase the values of $C_f \operatorname{Re}_x^{1/2}$. Meanwhile, the presence of slip parameter $(\gamma = 0.5)$ has reduced this physical quantity. It is due to slip effects has accelerated the fluid particle on surface to a certain velocity which is earlier obey the no slip conditions. This results to a decreasing in velocity differences which denoted as a reducing in velocity gradient as well as $C_f \operatorname{Re}_x^{1/2}$. It is worth mentioning here that the present of γ reduced $C_f \operatorname{Re}_x^{1/2}$ drastically which can be understood as the γ reduced the effects of stretching parameter ε on the skin friction coefficient $C_f \operatorname{Re}_x^{1/2}$.

CONCLUSIONS

The slip flow on a stagnation point past a stretching sheet in viscoelastic Walter's –B nanofluid model are solved numerically. It is shown how the pertinent parameters which are the Prandtl number Pr, the dimensionless viscoelastic parameter *K*, the stretching parameter ε, the Lewis number Le, the velocity slip parameter γ, and the Brownian N_b and thermophoresis motion parameter N_t affects the physical quantity discussed.

In summary, it is concluded that the Walter's fluid provide a better convective heat and mass transfer rate compared to a classical incompressible viscous fluid. Next, the presence of stretching effects enhanced the Nusselt number, Sherwood number and also the skin friction coefficient. Further, large values of Brownian and thermophoresis parameter may eliminate the convective heat transfer which promoted to the pure conduction process.

Lastly, it is suggested that the velocity slip effect is more significant at large values of viscoelastic parameter and stretching parameter. The presence of velocity slip parameter has accelerated the fluid particle at surface from static to a certain velocity. This situation reduced the skin friction coefficient. Further, it is found that the velocity slip parameter has also reduced the stretching parameters effect on the skin friction coefficient.

ACKNOWLEDGMENTS

The authors would like to thank the Universiti Malaysia Pahang for the financial and moral support in the form of research grant RDU140111 and RDU150101

REFERENCES

1. M. Turkyilmazoglu, *International Journal of Thermal Sciences* **50**(11), 2264-2276 (2011).
2. L. Crane, *Z. Angew. Math. Phys.* **21**, 645 - 647 (1970).
3. P. S. Gupta and A. S. Gupta, *The Canadian Journal of Chemical Engineering* **55**(6), 744-746 (1977).
4. T. C. Chiam, *Journal of the Physical Society of Japan* **63**, 2443-2444 (1994).
5. R. Nazar, N. Amin, D. Filip and I. Pop, *International Journal of Non-Linear Mechanics* **39**(7), 1227-1235 (2004).
6. A. Ishak, R. Nazar and I. Pop, *Acta Meccanica* **43**, 411-418 (2006).
7. A. Ishak, Y. Y. Lok and I. Pop, *Chemical Engineering Communications* **197**, 1417–1427 (2010).
8. Z. Abbas, Y. Wang, T. Hayat and M. Oberlack, *Nonlinear Analysis: Real World Applications* **11**(4), 3218-3228 (2010).
9. S. Motsa, Y. Khan and S. Shateyi, *Mathematical Problems in Engineering* **2012** (2012).
10. P. Ariel, T. Hayat and S. Asghar, *Acta Mechanica* **187**(1-4), 29-35 (2006).
11. T. Hayat, Z. Iqbal and M. Mustafa, *Journal of Mechanics* **28**(01), 209-216 (2012).
12. T. Hayat, S. Shehzad, A. Alsaedi and M. Alhothuali, *Chinese Physics Letters* **29**(11) (2012).
13. M. K. A. Mohamed, M. Z. Salleh, A. Ishak and I. Pop, *The European Physical Journal Plus* **130**(8), 1-9 (2015).
14. R. Nazar, M. Jaradat, N. Arifin and I. Pop, *Central European Journal of Physics* **9**(5), 1195-1202 (2011).
15. N. Bachok, A. Ishak and I. Pop, *Nanoscale Res. Lett.* **6** (2011).

16. P. Kameswaran, P. Sibanda, C. RamReddy and P. Murthy, *Boundary Value Problems* **2013**(1), 188 (2013).
17. M. K. A. Mohamed, N. A. Z. Noar, M. Z. Salleh and A. Ishak 2015. *AIP Proceedings of International Statistical Conference (ISM-II)*.
18. C. Sulochana and N. Sandeep, *Applied Nanoscience* **6**(3), 451-459 (2015).
19. S. Prabhakara and M. Deshpande, *Resonance* **9**(5), 61-71 (2004).
20. K. Bhattacharyya, S. Mukhopadhyay and G. C. Layek, *International Journal of Heat and Mass Transfer* **54**(1–3), 308-313 (2011).
21. S. K. Nandy and T. R. Mahapatra, *International Journal of Heat and Mass Transfer* **64**, 1091-1100 (2013).
22. K. Das, *Microfluidics and Nanofluidics* **16**(1-2), 391-401 (2014).
23. A. Malvandi, F. Hedayati and D. D. Ganji, *Powder Technology* **253**, 377-384 (2014).
24. H. Hashim, M. K. A. Mohamed, A. Hussanan, N. Ishak, N. M. Sarif and M. Z. Salleh 2015. *AIP Proceedings of The 2nd Innovation and Analytics Conference & Exhibition*.
25. J. Buongiorno, *Journal of Heat Transfer* **128**(3), 240-250
26. (2006).
27. C. Y. Wang, *International Journal of Non-Linear Mechanics* **43**(5), 377-382 (2008).
28. Y. Lok, A. Ishak and I. Pop, *Int. J. Numer. Methods Heat Fluid Flow* **21**, 61 - 72 (2011).
29. E. R. G. Eckert, *VDI Forsch.* **461** (1942).
30. M. Z. Salleh, R. Nazar and I. Pop, *Chemical Engineering Communications* **196**, 987-996 (2009).